International Journal of Nanoelectronics and Materials
Volume 11 (Special Issue) Dec 2018 [47-54]

Structural and Optical Properties of Co: ZnO Nanocomposite Thin Films Prepared by Spray Pyrolysis

Azhar I. Hassan[1*] and Intethar A. Hasson[1]

[1]*Laser Science, Applied science department, University of Technology, Baghdad, Iraq.*

ABSTRACT

Co: ZnO nanocomposite thin films were deposited on glass substrates by Spray pyrolysis at relatively low temperature of 350oC. X-ray diffraction, atomic force microscopy and UV–VIS optical spectrophotometry were used to characterize the structural and optical properties of the as-prepared nanocomposite thin films. X-ray diffraction patterns of the films showed that the films exhibited mixed structure of ZnO with hexagonal wurtzite structure and Co_3O_4 with cubic Spinal structure, and both crystalline structures have preferred orientation along (002) and (111) respectively. Topography of the films obtained by atomic force microscope revealed that the nanocomposite thin films have higher grain size and roughness in comparison with ZnO and Co_3O_4 thin films. The optical absorption spectra showed that the nanocomposite Co: ZnO films have lower transmittance than ZnO films and higher than Co_3O_4 films. Investigation of the optical absorption coefficient indicated that the adding of Co ratio leads to narrowing the band gap of the thin films from 3.2 to 2 eV.

Keywords: Nanocomposite Thin Films, Spray Pyrolysis, Zinc Oxide.

1. INTRODUCTION

Semiconducting materials which doped with magnetic transition metal like Fe, Co, Mn and Ni known as Diluted magnetic semiconductors (DMS) [1-2]. These types of semiconductor have received great attention recently because of their important applications in magneto electronic, spintronic and optoelectronic devices [3-5].

Zinc oxide is an II-VI group n-type semiconducting material holds a critical position because of its transparency in the visible range with wide band gap (~3.37 eV) and large exciton binding energy (60 meV) [6-7]. ZnO has massive applications in the fabrication of devices such as transparent high-power electronics, varistors, ultraviolet light-emitters, piezoelectric transducers, smart windows, gas-sensors and solar cells [8-13]. Zinc oxide has many advantages like low cost, abundance in nature, harm-lessens against environment and human being, high thermal and chemical stability [6,14-15]. Crystalline structure of ZnO mostly involves number of planes including tetrahedrally coordinated $O^{2-}$and Zn^{2+}ions, accumulated alternately along the c-axis [15]. ZnO alloying with transition metals as like cobalt (Co) has attracted of great interest because of the novelty of their fundamental properties [16]. Cobalt oxide is a p-type semiconductor has normal spinel structure, two energy band gaps (1.57 and 2.28) eV and have three kinds of the structure: Cobalt oxide Co_3O_4, Cobaltous oxide CoO and Cobaltic oxide Co_2O_3 [17-18]. It has been widely used as heterogeneous catalysts, magnetic materials, electrode materials and gas sensing materials [19-20]. In recent years, numerous techniques are performed to prepare ternary $Zn_{1-x}Co_xO$ thin films such as aerosol assisted chemical vapor deposition (AACVD), sol–gel, spray pyrolysis technique, laser molecular-beam epitaxy method, simple solution route and Pulsed Laser Deposition (PLD) [21-27].

* Corresponding Author: *Azhar.hassan@yahoo.com*

Until now spray pyrolysis method is infrequently used as deposition technique although it considered as a simple and comparatively low cost-effective technique [28]. Several studies depicted the growth processes of Co: ZnO thin film and showed the cobalt doping effect on the optical, structure, electrical, properties [29]. However, a few studies have focused on fabrication of CoZnO composite thin films at relatively low temperatures. In this study the structural, morphological and optical properties of ZnO, CoZnO, Co_3O_4 nanostructure thin films was studied using spray pyrolysis technique.

2. EXPERIMENTAL

The Co: ZnO thin film was deposited on a glass substrate using a laboratory spraying system. A precursor solution of 0.1M contains Zinc chloride ($ZnCl_2$) salt and cobalt chloride ($CoCl_2.6H_2O$) mixed with the different ratio of Co: ZnO (0, 40, 100) wt. % and then dissolved in distilled water. The glass substrates were cleaned carefully and sonicated in ethanol to remove the contamination from glass substrates. The solution was sprayed on the substrate at 350 ^oC. The solution flow rate was 5 ml/min, and the carrier gas was compressed air. The nozzle to substrate distance was 30 cm.

After the spraying process, the substrates were kept on the heater until cooled and reach room temperature to avoid the occurrence of any thermal stresses. X-ray diffractometer (XRD 6000, Shimadzu, Japan) with CuK_α line radiation (λ=1.5406 Å) was used to analysis the crystalline structure and phases. The morphology of prepared thin films was done by AFM (Ntegra NT-MDT). The spectral transmission was measured using UV-VIS spectrophotometer of (Shimadzu 3101 PC) type.

3. RESULT AND DISCUSSION

3.1 Structural Properties

The phases of the prepared thin films and their crystallographic orientation were identified by XRD analysis. X-ray spectrum for Co: ZnO thin films prepared at temperature 350^oC are presented in Fig. (1). The results pointed out that there is no unreacted phases of Zn and Co, thereby indicating that the Co dopant must be incorporated into the lattice as a substitutional atom. The presence of sharp peaks in XRD patterns demonstrates the polycrystalline nature of these ZnCoO thin films. (002) peak was indicating a strong orientation along the c-axis of ZnO with hexagonal wurtzite structure. The crystalline planes (100), (002), (101), (103), (102) all of the zinc oxide (ZnO) were apparent, and the preferred orientation is (002). This result is in agreement with the results of the published research [29]. The diffraction spectrum indicates that the intensity of the preferred orientation (002) decreases with loading of Co ratio.

At the Co loaded the emergence of new peaks of Co_3O_4 was observed that overlap with the ZnO peaks, especially at (101) diffraction peak, which has the highest density at ratio 0.6 cobalt due to the overlapping of (311) peak of the Co_3O_4 with the (101) peak of the ZnO and this referred the formation of nanocomposite thin film. So, the ratio of (0.4) represents the mixing case of the materials because of the cobalt ion (Co^{+2}) replacement with zinc ions (Zn^{+2}) in the crystalline lattice. This may be attributed to the small difference between the ionic diameters of cobalt ions Co^{+2} (0.69 nm) and zinc ions Zn^{+2} (0.74) [30]. The cobalt ion has started to enter the zinc lattice in two ways, namely the substitution and the interstitial, which led to the formation of the Co_3O_4 and this agreement with the research [25].

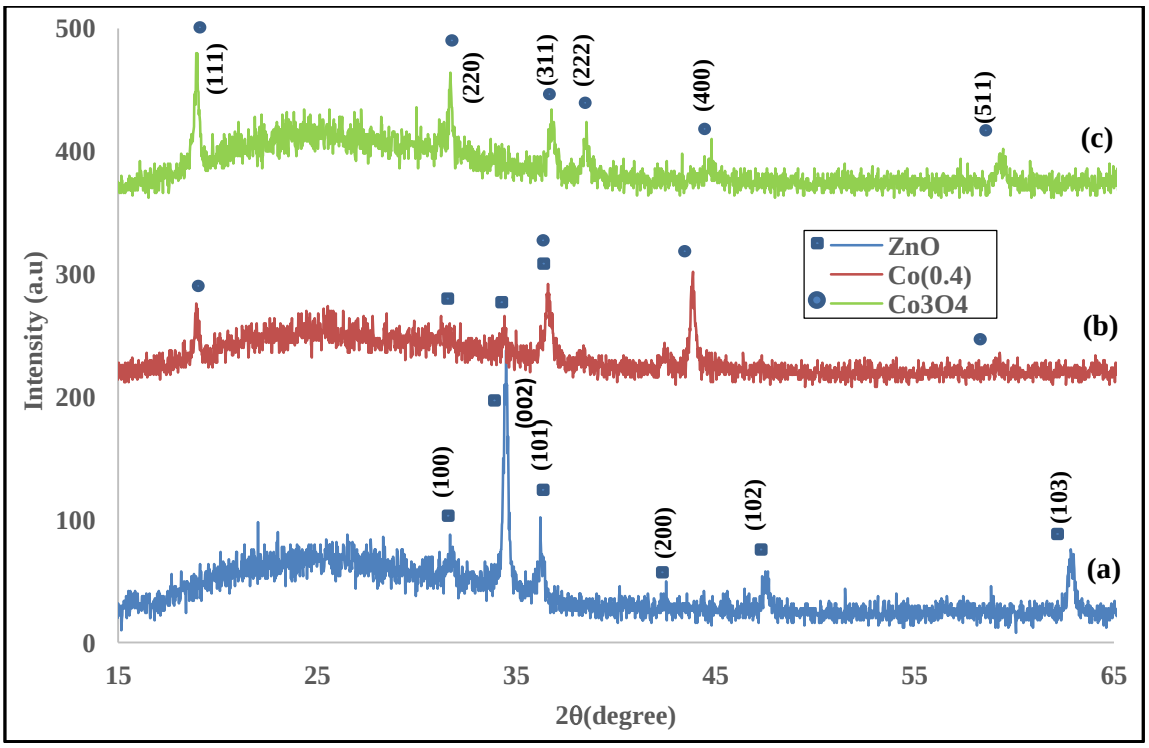

Figure 1. XRD pattern of the Co:ZnO thin film deposited on glass at 350 °C, (a) ZnO, (b) $Co_{0.4}Zn_{0.6}O$, (c) Co_3O_4.

Figure 1 indicate that Co_3O_4 thin film has a polycrystalline spinel cubic structure at peaks orientation (111), (220), (311), (222) and (400) planes with the preferred orientation of (111) plane and this agrees with Louardi [19]. The positions of the XRD peaks of the sample correctly match the standard PDF values (ICDD -International Crystal diffraction data) No. 042-1467 for cobalt oxide and 36-1451 for zinc oxides.

Crystalline size of Co: ZnO nanocomposite thin films was estimated using Scherer's Equation $D=0.9\lambda/\beta\cos\theta$, where the shape factor is K = 0.94, λ is the wavelength of X-rays (1.5406 for Cukα), θ is the Bragg's angle, β is the full width at half maximum [26]. It can be noticed from table (1) that the crystallite size changed with loading of cobalt. The existence of Co ions prevent and restricted the crystal growth, and the decreasing in crystallite size with Co content indicates that the increment of Co-benefits the crystallite size reduction.

The values of the crystalline size are found to be varied between 33 and18 nm as Co loaded suggesting the formation of nanostructured CoZnO thin film. The lattice constant for (002) and (101, 311) peaks of the ZnO and Co: ZnO thin films are shown in the table (1). The value of lattice constant for pure ZnO (a, c) are (3.4979, 5.2005) A° respectively which agreement with [6], while the value of a cubic Co3O4 lattice constant (a) for (111) plane is 8.095A° as shown in [20]. The adding of cobalt rarely increases the lattice constant of the Co:ZnO thin films with respect to that the volume of Co^{2+} in the tetrahedral composition has a 0.69nm Ionic radius close to that of Zn^{2+} which is equal to 0.74 nm[30], thus zinc ions are regularly replaced by cobalt ions.

Figure 2 represents the AFM micrographs image of pure and Co-loaded ZnO films. The figure show nanostructure and uniform surface, and self-assembly of particles as spherical and rod formation with the existence of Co. Table 2 represent the value of grain size, roughness average and RMS of Co:ZnO surface nanocomposite thin films is obtained from the image of 2×2 μm scanning area. It is clear that the grain size is increase with Co because the content of Zn^{2+} which

have the larger ionic radius is greater than Co^{2+} content and then the grain size begin to decrease due to the overcome of cobalt that has smaller radius.

Table 1 XRD data for the Co:ZnO nanocomposite thin films

	2Θ (deg)	**hkl**	**d (Å)**	**FWHM (deg)**	**Crystalline size D nm**	**Lattice constant (c) (ZnO)**	**Lattice constant (a) (ZnO)**	**Lattice constant (a)(Co_3O_4)**
ZnO	34.47	(002)	2.5995	0.257	33.76	5.2005	3.4979	-
Co:ZnO	36.6	(101)	2.452	0.35	24.97	5.215	3.01	-
	36.6	(311)	2.452	0.35	24.97	-	-	8.1323
Co_3O_4	18.98	(111)	4.6699	0.298	18.16	-	-	8.095

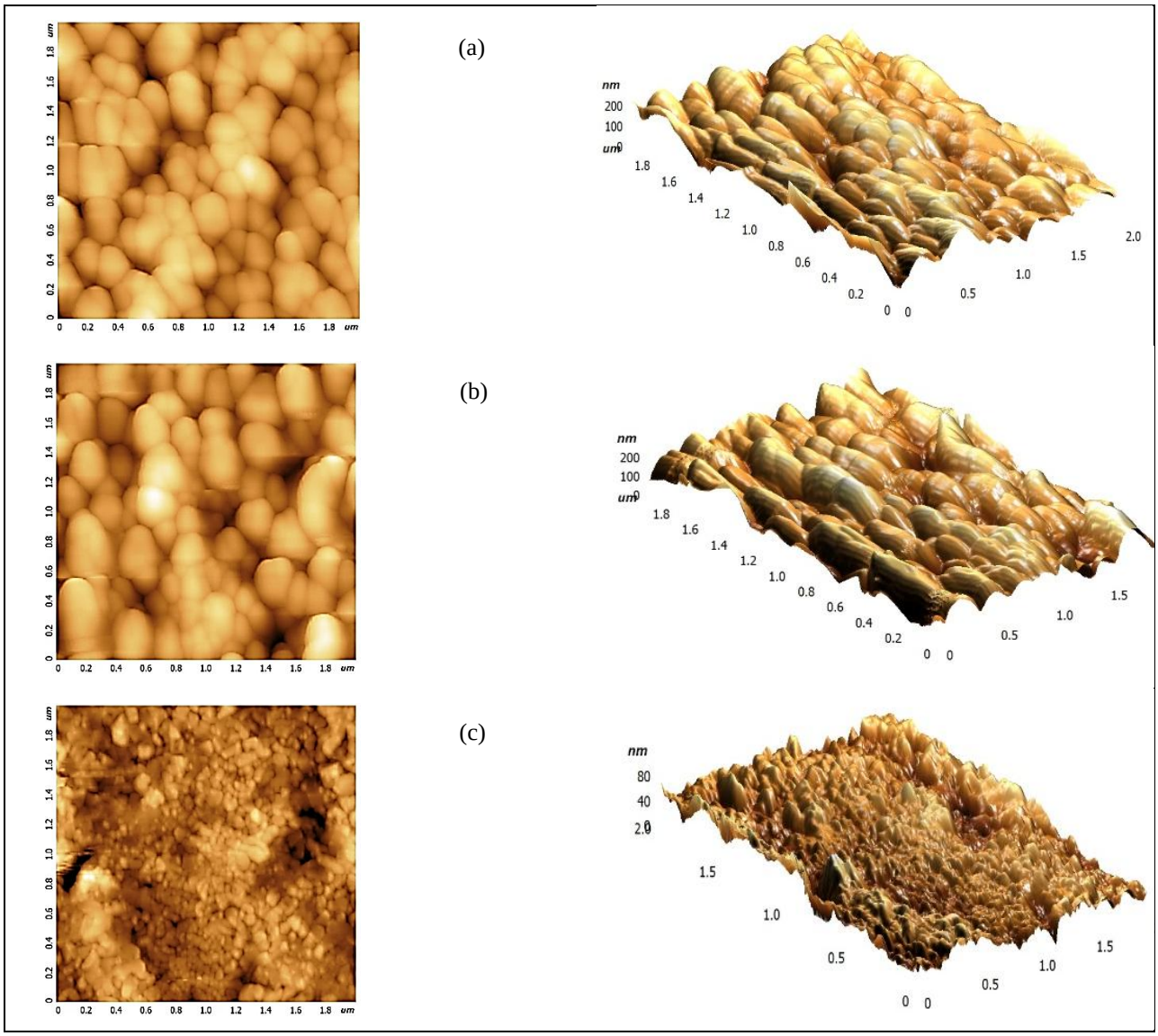

Figure 2. 3-D AFM image of a-ZnO, b- Zn0.6Co0.4O and c- Co_3O_4 thin film deposited on glass at 350 ^oC.

Table 2 Grain size, Roughness average and RMS of Co: ZnO nanocomposite thin films measured from AFM image

	Grain size (nm)	Roughness Averag (nm)	Roughness RMS (nm)
ZnO	130	30.344	38.947
Co:ZnO	158	51.601	63.175
Co_3O_4	42.8	19.684	24.542

3.2 Optical Properties

The transmission measurement and the estimated absorption coefficient could be shown in Figure 3. Figure 3a represent the variation of the optical transmission spectra with the incident wavelength for the Co: ZnO thin films. It is clear that the optical transmittance in the visible region was increase while in the ultraviolet region was decrease for all thin films.

The loading of Co concentration caused a gradual decrease in the transmittance spectra, and there is an altered in the band edge towards the longer wavelength side. This red shift of edge band emission asserts that the band gap of Co: ZnO thin films decrease with the Co content. The films with Co ratio show two absorption peaks which attach with d-d electron transition of Co^{2+} in the tetragonal crystal structure. This supposes that Co^{2+} replace Zn^{2+} in the lattice substitutionally due to the low difference between their ionic radiuses as mention above.

The absorption coefficient (α) can be calculated by using the well-known formula [27], α = (1/t) ln (1/T), Where (t) is a thickness of thin film, T= is a transmittance. The relation of the absorption Coefficient (α) against photon energy (hν) for Co: ZnO thin films are shown in Fig. (3b).

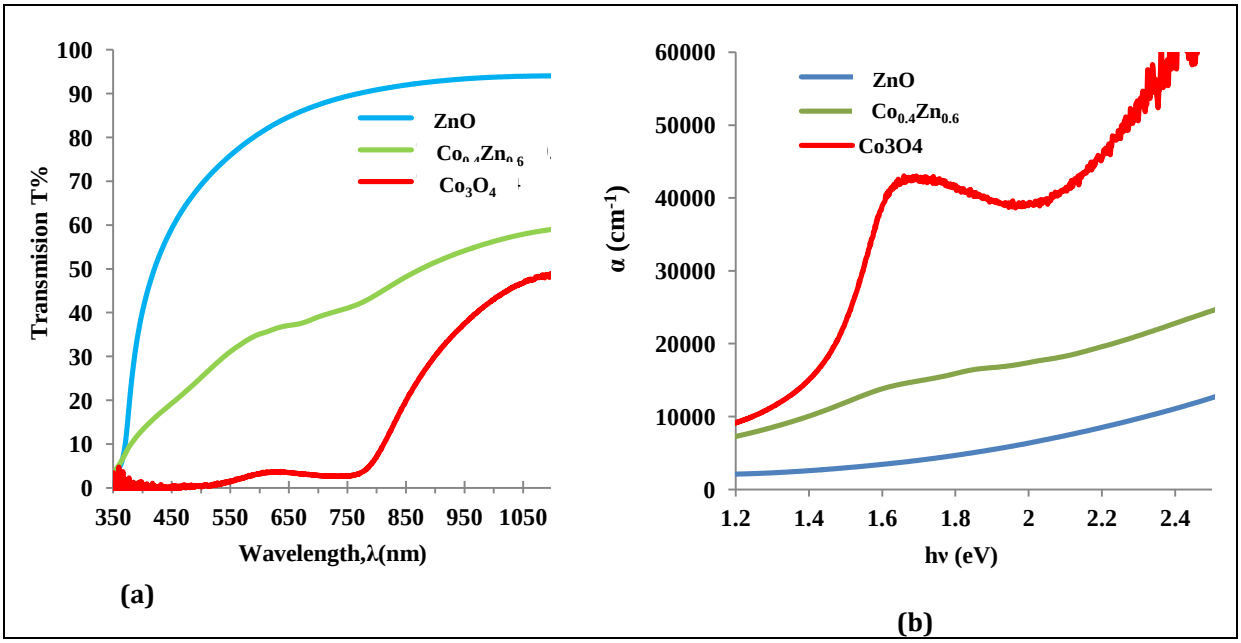

Figure 3. The optical transmission spectra (a) and Absorption coefficient spectra (b) of Co: ZnO nanocomposite thin films.

It can be notice that the absorption coefficient gradually increasing with photon energy. Also, there is a sharp absorption edge in the visible region for all films. This indicates that the

absorption band gap transitions in pure ZnO and substituted cobalt oxide thin films are direct. But for films with Co ratio, there is two absorption edge in the absorption coefficient spectra which indicating that Co^{2+} is substituted with Zn^{2+} in ZnO lattice .

The optical energy gap (Eg) of thin films was deduced by plotting (αhν) 2 with hν as shown in Fig. (4), where hν is the photon energy. The optical energy gaps of the Co: ZnO samples show that the band gap of ZnO can be varied by Co doping as shown in table (3), which show that the estimated energy gap values are decrease with Co content. The addition of cobalt content will produce an defects inside zinc oxide structure, this defects will create an localized states and hence decreased the energy gap value.

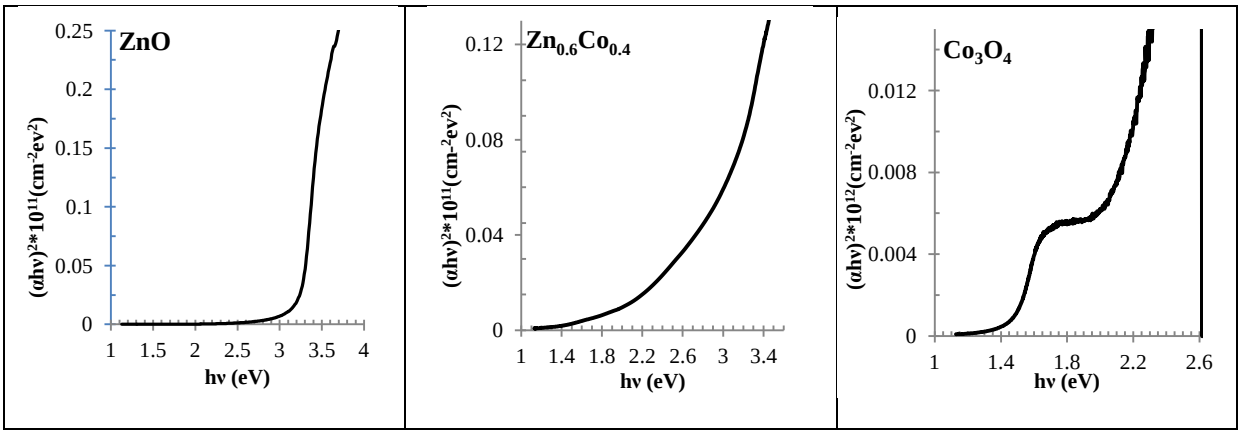

Figure 4. (αhν)2 versus hν plots of Co:ZnO thin films.

The low-energy shift of energy gap with Co concentration can be clarify with two reasons: (i) it might result from destabilization of O^{2-} (2p6 orbitals at O^{2-} ions adjacent to Co^{2+}), which extends the valence band edge by 0.5 eV, or point defects as like nanoclusters of CoZnO; (ii) as mainly due to the s-d and p-d spin-exchange interactions between band electrons and localized d-electrons of Co^{2+} ions substituting Zn^{2+} ions[1].

The band gaps of Co_3O_4 thin films are 1.48 eV in the lower energy region and 2eV for higher energy region, which are consistent with the reported Co_3O_4 band structure. The energy of 2 eV is assigned to the charge transfer transition between the p states of O^{2-} and the d states of Co^{2+}.

Table 3 Energy band gap data of Co:ZnO nanocomposite thin films

	ZnO	**Co: ZnO**	**Co_3O_4**
Energy gap (eV)	3.2	2.8	2, 1.48

4. CONCLUSION

Nanocomposite Co: ZnO thin films were deposited successfully by spray pyrolysis method on glass substrate at temperature of 350°C. The XRD patterns confirmed the existence of a hexagonal wurtzite structure and spinal cubic structure for both ZnO and Co_3O_4 thin films and the existing of cobalt is affected directly on the formed phases. The highest transmittance (80%) was observed in the near-infrared region of the electromagnetic spectrum. The optical properties results show the ability to control direct optical band gap energy by Co ratio, which decreases from 3.2 to 2 eV with Co concentration.

ACKNOWLEDGMENTS

This work was supported by Laser Science Branch- Department of Applied Science at the University of Technology and the authors are thankful to the staff of the NanoLAB at the Center of Advance Material for their help in microscopy analysis and for useful discussions.

REFERENCES

[1] Savchuk, A. I., Stolyarchuk, I. D., Stefaniuk, I., Cieniek, B., Sheregii, E., Semiconductor Physics, Quantum Electronics & Optoelectronics **17**, 4 (2014) 353-357.
[2] Kayani, Z. N., Ishaque, R., Zulfiqar, B., Riaz, S., Naseem, S., Opt. Quant Electron **49** (2017) 223.
[3] Bhat, T. M., Gupta, D. C., J. Physics and Chemistry of Solids **112** (2018) 190-199.
[4] Fouchet, A., Prellier, W., Méchin, L., Superlattices and Microstructures **42**, 1–6 (2007) 185-190.
[5] Sun, H., Uang Jen,S., Pang Chiang, H., Chi Chen, S., Huei Lin, M., Yu Chen, J., Wang, X., Thin Solid Films **641**, 1 November (2017) 12-18.
[6] Kahraman, S., Çetinkara, H. A., Bayansal, F., Çakmak, H. M., Güder, H. S., Philosophical Magazine **92**, 17 (2012) 2150–2163.
[7] Zhang, H. Z., Sun, X. C., Wang, R. M., Yu, D. P., J. Crystal Growth **269** (2004) 464–471.
[8] Marouf, S., Beniaiche, A., Kardarian, K., Mendes, M. J., Sanchez-Sobrado, O., Águas, H., Fortunato, E., Martins, R., Analytical and Applied Pyrolysis **127** (2017) 299-308.
[9] Zhao, H., Hu, J., Chen, S., Xie, Q., He, J., Ceramics International **42**, 15 (2016) 17880-17883.
[10] Chen, C., Zhang, J., Chen, J., Wang, S., Chen, C., Materials Letters **189**, 15 February (2017) 144-147.
[11] Ambersley, M. D., Pitt, C. W., Thin Solid Films **80**, 1–3 (1981) 183-195.
[12] Zhao, Y., Xu, R., Zhang, X., Hu, X., Lu, Y., Energy and Buildings **66** (2013) 545-552.
[13] Zhu, L., Zeng, W., Review article, *Sensors* and Actuators A: Physical **267** (2017) 242-261.
[14] Ravichandrana, K., Dineshbabua, N., Arunb, T., Manivasahama, A., Sindhuja, E., J.Applied Surface Science **392** (2017) 624-633.
[15] Kaura, M., Kailasaganapathia, S., Ramgira, N., Dattaa, N., Kumarb, S., Debnatha, A. K., Aswala, D. K., Guptaa, S. K., Applied Surface Science **394** (2017) 258–266.
[16] Samanta, K., Bhattacharya, P., Katiyar, R. S., J. Physical Review B **75** (2007) 035208,.
[17] Manickam, M., Ponnuswamy, V., Sankar, C., Suresh, R., Optik - International Journal for Light and Electron Optics (2016).
[18] Azhar, I. H., Maki, S. I., Energy Procedia **119** (2017) 961–971.
[19] Louardi, A., Rmili, A., Chtouki, T., Elidrissi, B., Erguig, H., El Bachiri, A., Ammous, K., Mejbri, H., **8**, 2 (2017) 485-493.
[20] Lohaus, C., Morasch, J., Brötz, J., Klein, A., Jaegermann, W., J. Phys. D: Appl. Phys. **49** (2016) 155306.
[21] Basit, M., Shah, N. A., Ali, S. M., Zia, A., World Applied Sciences **32**, 8 (2014) 1664-1670.
[22] Gungora, E., Gungora, T., Caliskanb, D., Ceylanc, A., Ozbay, E., Applied Surface Science **318** (2014) 309–313.
[23] Saha, S. K., Rahman, M. A., Sarkar, M. R. H., Shahjahan, M., Khan, M. K. R., Semiconductors **36** (2015) 3, 1-6.
[24] Kayani, Z. N., Ishaque, R., Zulfiqar, B., Riaz, S., Naseem, S., Opt Quant Electron **49** (2017) 223.
[25] Jin, Z., Fukumura, T., Kawasaki, M., Applied Physics Litters **78**, 24 (2001) 3824-3826.
[26] Sharma, N., Thakur, S., Sharma, R., Kumar, J., CPUH-Research Journal 1 (2015) 47-51.
[27] Ivill, M., Pearton, S. J., Rawal, S., Leu, L., Sadik, P., Das, R., Hebard, A. F., Chisholm, M., Budai, J. D., Norton, D. P., Physics **10** (2008) 065002.

[28] Pavan, M., Rühle, S., Ginsburg, A., Keller, D. A., Noa Barad, H., Sberna, P. M., Nunes, D., Martins, R., Anderson, A. Y., Zaban, A., Fortunato, E., Solar Energy Materials & Solar Cells **132** (2015) 549–556.
[29] Singh, G., Shrivastava, S. B., Ganesan, V., Chem. Eng. Mater. Sci. **4**, 1 (2013) 1-6.
[30] Chtouki, T., Louardi, A., Elidrissi, B., Erguig, H., Materials Science and Engineering **A3**, 11 (2013) 743-750.